Functional Copolymer/Organo-MMT Nanoarchitectures. II. Dynamic Mechanical Behavior of Poly(MA-co-BMA)s-organo-MMT Clay Nanocomposites

Zakir M. O. Rzayev,[1] Ali Güner,[2] Ernur A. Söylemez,[1] Serap Kavlak[2]

[1]*Department of Chemical Engineering, Faculty of Engineering, Hacettepe University, Beytepe, 06800 Ankara, Turkey*
[2]*Department of Chemistry, Faculty of Science, Hacettepe University, Beytepe, 06532 Ankara, Turkey*

Received 9 June 2009; accepted 6 April 2010
DOI 10.1002/app.32606
Published online 30 June 2010 in Wiley InterScience (www.interscience.wiley.com).

ABSTRACT: Functional copolymer/organo-silicate [*N,N′*-dimethyldodecyl ammonium cation surface modified montmorillonite (MMT)] layered nanocomposites have been synthesized by interlamellar complex-radical copolymerization of preintercalated maleic anhydride (MA)/ organo-MMT complex as a 'nano-reactor' with *n*-butyl methacrylate (BMA) as an internal plasticization comonomer in the presence of radical initiator. Synthesized copolymers and their nanocomposites were investigated by dynamic mechanic analysis, X-ray diffraction, SEM, and TEM methods. It was found that nanocomposite dynamic mechanical properties strongly depend on the force of interfacial MA...organo-MMT complex formation and the amount of flexible *n*-butyl ester linkages. An increase in both of these parameters leads to enhanced intercalation and exfoliation *in situ* processes of copolymer chains and the formation of hybrid nanocomposites. © 2010 Wiley Periodicals, Inc. J Appl Polym Sci 118: 2904–2913, 2010

Key words: synthesis; modified organoclay; nanocomposites; structure-property relations

INTRODUCTION

In the last decade, the alternating, random and graft copolymers of maleic anhydride (MA) and its isostructural analogues were widely utilized for the preparation of polymer/organo-silicate (or silica) hybrid materials through melt compounding by reactive extrusion and sol–gel methods. However, interlamellar copolymerization of MA and its preintercalated complexes with organo-clays, and MA copolymer/organoclay composition–nanostructure–property relationships have not been investigated. Synthesis and characterization of some selective functional copolymer/organo-silicate or silica hybrid nanocomposites were a subject of our previous publications.[1–5] Although the most promising reaction to great polymer/clay nanocomposites is the polymerization of functional monomers, such as styrene,[6–8] *N*-vinylcarbazole,[9] 4-vinylpyridine,[10] methyl methacrylate,[11–15] acrylonitrile,[16] and *N*-*n*-butylmaleimide,[17] the intercalative radical copolymerization of binary or ternary monomer systems in the presence of mineral clay has been scarcely investigated. Examples are bulk copolymerization of styrene–methyl methacrylate,[18–20] emulsion copolymerization of styrene–acrylonitrile,[21] styrene–*N*-phenylmaleimide (PhMI),[22] and styrene–butyl methacrylate[23] monomer pairs. It was observed that the polymerization rate accelerated by the addition of clay in reaction medium; this addition also significantly influenced the structure and properties of the prepared polymer nanocomposites.[8–24] Liu et al.[14,25,26] investigated the bulk, solution and emulsion copolymerization of styrene with methyl methacrylate and PhMI (at 1 : 9 molar PhMI/ styrene feed ratio) in the presence of organo(cetyltrimethyl ammonium bromide)-modified montmorillonite (MMT) clay or Na^+-MMT to prepare nanocomposites with good dispersability of clay. Wang et al.[27,28] showed that a comparison of solution, emulsion, suspension, and bulk polymerization along nanocomposites may also be prepared by melt *in situ* reactive blending of monomer/polymer/clay mixtures. In recently published review article of Tjong,[29] current development on the processing, structure, and mechanical properties of polymer nanocomposites reinforced with respective layered silicates, ceramic nanoparticles, and carbon nanotubes were described. Author paid particular attention to the structure–property relationship of such novel high performance polymer nanocomposites. Nguen and Baird[30] reported the different methods and types of polymers used for preparation of polymer nanocomposites, the structure and properties of layered silicates, and the most common techniques

Correspondence to: Z. M. O. Rzayev (zmo@hacettepe.edu.tr).

used for characterization of nanocomposites. Heinz et al.[31] investigated the structure and dynamics of alkyl ammonium-modified MMT clays with different cation exchange capacity (CEC), ammonium head groups, and chain length by computational molecular dynamics simulation for a large set of structures and compared to a wide array of experimental data (X-ray, IR, NMR, and DSC). They found that the relationship between computational and experimental data is very complementary in the 44 various organo-MMT systems. According to the authors, the size of the computational data set surpasses prior to experimental work in the area and will provide guidance in the choice of alkyl modifiers for interactions with solvents, polymers, and other nanoscale building blocks.

In this work, the synthesis and dynamic mechanic behavior of silicate layered nanocomposites such as poly(maleic anhydride-*co*-*n*-butylmethacrylate)s/*N*, *N*′-dimethyl dodecylamine modified MMT [poly (MA-*co*-BMA)/DMDA-MMT] have been described. Nanocomposites were prepared by the complex-radical interlamellar copolymerizations of preintercalated MA...organo-MMT monomer complex with different amounts of BMA comonomer in methyl ethyl ketone (MEK) at 65°C under nitrogen atmosphere. The obtained thermal behavior, especially glass transition temperature (T_g), and dynamic mechanical parameters of the virgin copolymers and their nanocomposites have been discussed as a function of the effective intercalation/exfoliation of the copolymer chains and formation of nanostructure. General scheme for the synthesis of poly(MA-*co*-BMA)s/DMDA-MMT nanostructures via complex formation and interlamellar copolymerization can be represented as follows (Scheme 1).

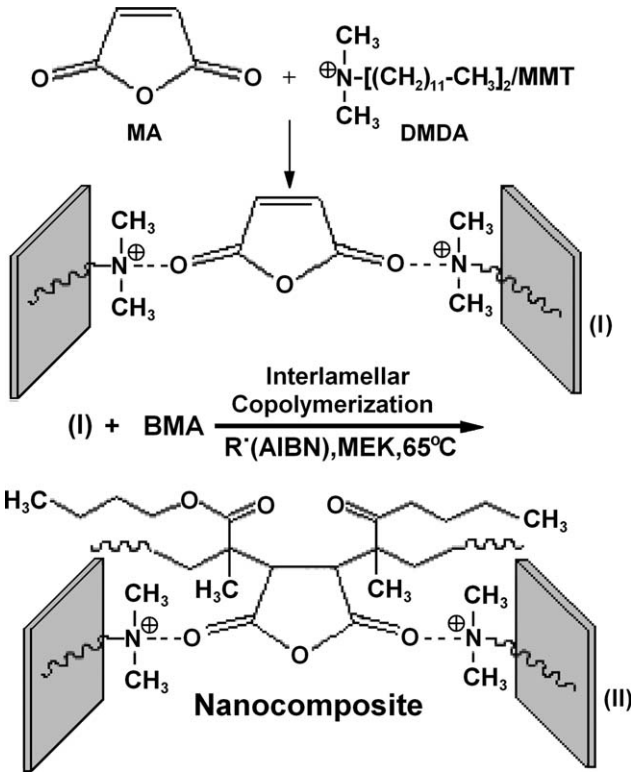

Scheme 1 Interlamellar complex-radical copolymerization of monomer complex of MA...DMDA-MMT clay with *n*-butyl methacrylate (BMA): (I) structure of preintercalated monomercomplex and (II) poly(MA-*co*-BMA)/O-MMT nanocomposite.

EXPERIMENTAL

Materials

BMA monomer (Aldrich-Sigma, Germany) was purified before use by distillation under moderate vacuum. MA monomer (Fluka, Switzerland) was purified by recrystallization from anhydrous benzene solution through sublimation in vacuum. The α,α′-azoisobutyronitrile (AIBN) (Fluka) was recrystallized twice from methanol solution. DMDA-MMT orgnoclay was obtained from Bensan (Enez, Turkey). Full characteristic parameters of this organoclay were presented in our recently published works.[1,2] All other solvents and reagents were of analytical grade and used without purification.

Synthesis of MA...DMDA-MMT complex

MA monomer was dispersed in methyl ethyl ketone (MEK)/DMDA-MMT mixture at monomer/*N*,*N*′-dimethyldodecyl ammonium molar ratio of 1 : 2 by intensive mixing at 50°C for 3 h to prepare the intercalated complex of MA with DMDA-MMT. Then the prepared mixture was treated by a lage amount of methanol at 20°C by intesive mixing up to full precipitation of powder product, which is isolated by filtration, and drying under vacuum.

Synthesis of poly(MA-*co*-BMA)s

Synthesis of poly(MA-*co*-BMA)s containing different amounts of flexible BMA units was carried out by copolymerization of MA and BMA using various molar monomer ratios of MA : BMA = 1 : 1 (1 : 2 and 1 : 3) in MEK with AIBN as an initiator at 65°C under nitrogen atmsphere. Reaction conditions: $[M]_{total}$ = 2.7 mol L^{-1}, [AIBN] = 2.03 × 10^{-2} mol L^{-1}, [MEK]/[M] = 3, molar monomer ratios of MA/BMA = 1.0, 0.33, and 0.2, reaction time 24 h, and conversion around 65–78 wt %. Copolymerizations were carried out in a carousel type Pyrex-glass microreactor with a thermostated heater and magnetic mixer. The copolymers were isolated from reaction mixture by precipitating with diethyl ether, then washed with several portions of benzene and dried at 50°C under vacuum.

TABLE I
Composition and Some Properties of Poly(MA-*co*-BMA)s

Copolymers	AN (mgKOH/g)	Content of BMA unit (mol %)	T_g (°C) (by DMA)	$[\eta]_{in}$ (dL g^{-1}) in MEK at 25 ± 0.1°C
Poly(MA-*co*-BMA)-1	389.0	57.2	60.1	0.23
Poly(MA-*co*-BMA)-2	122.1	85.2	60.3	0.27
Poly(MA-*co*-BMA)-3	66.4	91.8	57.7	0.29

Interlamellar copolymerization procedure

An appropriate amount of BMA monomer and AIBN was added to reaction mixture containing given amounts of MA...Organo-MMT complex dispersed in MEK and heated with intensive mixing at 65°C under nitrogen atmosphere for 24 h. Prepared hybrid composition was isolated by precipitation with methanol, then washed with several portions of diethyl ether and benzene, and dried under vacuum at 60°C.

Characterization

Dynamic mechanic analysis of synthesized copolymers and their nanocomposites was performed with Dynamic Mechanic Analyzer (TA Instruments, Q800). Powdered mixtures of polymer and Al_2O_3 (50 : 50 wt %) were loaded into the DMA using powder-holder. The holder was clamped directly into the DMA dual cantilever. The temperature dependence of polymers was measured at a constant frquency of 1 Hz and a heat rate of 3°C/min.

Acid number (AN, mgKON/g) of poly(MA-*co*-BMA)s containing anhydride groups was determined by standard titration method. The copolymer compositions were calculated using chemical analysis data (acid number for MA units, Table I) and the following equation:

$$m_1(\text{mol }\%) = W_2/[2M_{(\text{KOH})}/\text{AN} - (W_1 - W_2)] \times 10^{-2}, \quad (1)$$

where W_1 and W_2 are molecular weights of m_1 and m_2 ($m_1 + m_2 = 1$) monomer units, AN is acid number (in g KOH/g) and $M_{(\text{KOH})}$ is molecular weight of KOH.

Intrinsic viscosities of poly(MA-*co*-BMA)s with different compositions were determined in MEK at 25 ± 0.1°C within the concentration range of 0.01–1.5 g dL^{-1} using an Ubbelohde viscometer.

The X-ray powder diffraction (XRD) patterns were obtained from a Rigaku D-Max 2200 powder diffractometer. The XRD difractograms were measured at 2θ, in the range 1°–50°, using a CuK_α incident beam ($\lambda = 1.5406$ Å), monochromated by a Ni-filter. The Bragg equation was used to calculate the interlayer spacing (d): $n\lambda = 2d\sin\theta$, where n is the order of reflection, and θ is the angle of reflection. Crystallinity of the nanocomposites (χ_c) was calculated using the following eq. (2):

$$\chi_c(\%) = W_c/(W_c + W_a) \times 10^{-2}, \quad (2)$$

where W_c and W_a are the areas of the crystalline and amorphous portions in the X-ray diffractogram, respectively.

Intercalation/exfoliation degree (ED) was calculated according to the eq. (3):

$$\text{ED}(\%) = I_e/(I_e + I_o) \times 10^{-2}, \quad (3)$$

where I_e (or I_c) and I_o are the intensity of the diffraction peaks associated with the exfoliated (or intercalated) and nonexfoliated structures at corresponding 2θ values.

The surface morphology of nanocomposites was examined using a scanning electron microscope (JSM-6400 JOEL SEM with scale: 1 and 10 μm, $\times 10^4$ and an accelaration voltage 20 kV). All specimens were freeze-dried and coated with a thin layer of gold before testing. Transmission electron microscopy (TEM) images were obtained on a JEOL JEM-2100F transmission electron microscope with an acceleration voltage of 200 kV and emission current 146 mA. This method allowed to perform a higher resolution image due to the decrease in wavelength. An electron gun emits an electron beam which moves through a condenser aperture and then bombards the specimen. The TEM specimens were cut at room temperature using an ultra microtome. Thin specimens, 50–80 nm, were collected in a trough filled with water and placed on 200 mesh copper grids.

RESULTS AND DISCUSSION

Composition and properties of copolymers

The composition and some properties of synthesized copolymers containing various amounts of BMA units are summarized in Table I. These copolymers were synthesized using different monomer feed molar ratios ([MA] : [BMA] = (1 : 1, 1 : 2, and 1 : 3). As seen from Table I, increase in content of the BMA units in copolymers provides a visible decrease in T_g values and increase in intrinsic

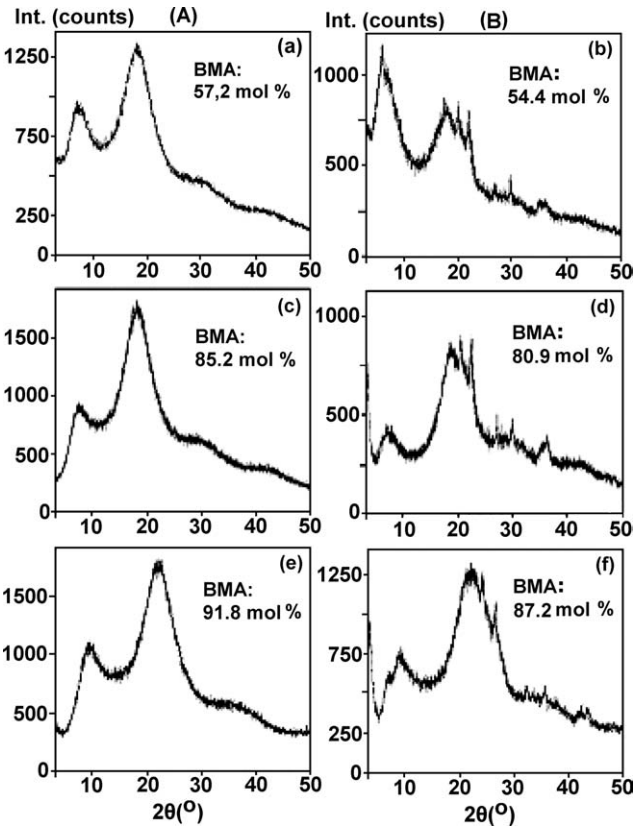

Figure 1 XRD spectra of **A:** poly(MA-*co*-BMA)s containing (a) 57.2, (b) 85.2, and (c) 91.8 mol % of BMA unit; **B:** poly(MA-*co*-BMA)s/O-MMT nanocomposites with (a) 54.4, (b) 80.9, and (c) 88.2 mol % of BMA unit.

viscosity, and therefore increase of average viscosity molecular weights (M_v) of the copolymers.

X-ray diffraction parameters

Physical structure of synthesized preintercalated MA...O-MMT monomer complex and poly(MA-*co*-BMA)s/O-MMT nanocomposites were investigated by XRD analysis method. Obtained results of XRD analysis of complex, pristine O-MMT, and nanocomposites were illustrated in Figure 1 and summarized in Table II. As seen from these data, $d_{(001)}$ and $d_{(002)}$ values for crystallographic planes depending on the interlamellar complex formation and exfoliation of copolymer chains into the silicate lamellae. Better intercalation is evidenced by the shift of 2θ values to the lower region (from 3.62° for pristine organoclay to 2.54° for MA...DMDA monomer complex) and increasing $d_{(001)}$-spacing parameters from 24.38 to 34.77 Å, respectively. Taking into consideration that the surface area of organoclay is modified by DMDA at approximately 30%, intercalation degree (ID) of a complexed MA monomer can be estimated to be approximately 95.0% for $d_{(001)}$ and ~ 100 % for $d_{(002)}$, respectively.

The results of XRD analysis of nanocomposites (Table II) show the following changes in XRD spectra: (1) disappearance of peaks at 2θ 5.20° (d = 16.98 Å) and 8.94° (d = 9.88 Å) and exfoliation of the silicate lamellae in XRD spectra of nanocomposites relating to 1 : 2 layered structure in pristine DMDA-MMT clay, (2) essential shift of characteristic peaks at 2θ from 3.62° to lower region of 2.04° which is accompanied with an increase of $d_{(001)}$ value from 24.38 Å for pristine organoclay to around 32.81–36.05 Å for nanocomposite. Increase of flexible butyl ester side-chain linkages provides relatively easy exfoliation process of copolymer chains unlike decreasing MA complexed organoclay in the feed copolymerizing mixtures, and (3) the formation of semicrystalline structure in nanocomposites unlike full amorphous structure of virgin copolymers (Fig. 1). These observed facts allowed us to propose that the interlamellar copolymerization of MA...O-MMT with BMA comonomer was predominantly carried out through exfoliation of copolymer chains due to effects of interfacial interaction and internal plasticization of branched *n*-butyl ester linkages. The crystallinity (χ_c) visibly increases with increasing content

TABLE II
XRD Parameters of Preintercalated [MA...O-MMT] Complex, Copolymers/O-MMT Nanocomposites, and Pristine O-MMT

Monomer complex and its nanocomposites	2θ (°)	*d*-spacing (Å)	Intensity (counts)	ID/ED (%)	χ_c (%)
[MA...O-MMT] complex	2.54	34.77	2395	57.02	56.2
	4.72	18.71	1081	58.85	
Poly(MA-*co*-BMA)(1 : 1)/O-MMT	2.38	37.11	1511	45.57	30.4
	–	–	0	100	
Poly(MA-*co*-BMA)(1 : 2)/O-MMT	2.52	35.06	1006	35.78	35.3
	–	–	0	100	
Poly(MA-*co*-BMA)(1 : 3)/O-MMT	2.45	36.05	955	34.60	36.5
	–	–	0	100	
Pristine O-MMT	3.62	24.38	1805	25–30[a]	58.1
	5.20	16.98	736	30–35[a]	

[a] These values were calculated from comparative analysis of nonmodified MMT and O-MMT using eq. (3).

of the flexible BMA linkages in nanocomposites, in spite of the decreasing content of the complex-forming MA units. This phenomenon may be explained by the effect of side-chain *n*-butyl ester on the local chain folding and crystallization process in the copolymer matrix.

Dynamic mechanical behavior

Dynamic Mechanical Analysis (DMA) method allows to determine the loss tan δ, the storage modulus (G') and the loss modulus (G'') as a function of temperature. The loss tan δ is equal to the ratio of G''/G', which exhibits the higher response to the chemical and physical structural changes and phase transitions of polymer system; the storage modulus G' is associated with the elastic modulus of the polymer or its composite; the loss modulus G'' is related to the energy loss (damping factor) as a result of the friction of polymer chain movement. It is known that the decrease of G' is less dependent on the temperature changes and this process as a function of temperature very slowly proceeds in polymer system due to increased polymer chain mobility and flexibility.[32] Generally, this process continues until the glass transition region is approached, and then G' decreases rapidly. In this isothermal condition, both the loss modulus G'' and loss tan δ increase and go via a maximum. The glass transition temperature (T_g) is determined as the temperature at which a maximum of loss tan δ is observed. This is a well known and much more an exact method for determining T_g values of polymers and their composites.[33] The glass transition of polymer materials can be broadened or shifted through various chemical and physical means.[34] Masenelli-Varlot et al.[35] proposed an interpretation of the DMA spectra, according to the intensity of the interfacial adhesion strength which directly influences the intensity of the reinforcement above T_g. This principle can also be used to characterize the microstructure of functional copolymer/organo-MMT nanocomposites in terms of interfacial adhesion strength. The results of the comparative DMA analysis of pure poly(MA-*co*-BMA)(1 : 1) and poly(MA-*co*-BMA)(1 : 1)/Organo-MMT nanocomposites, and DMA parameters as functions of temperature and content of flexible BMA unit are illustrated in Figure 2.

The obtained results indicate the following changes in DMA curves when copolymer is exfoliated between organo-silicate layers by interlamellar complex-radical copolymerization of preintercalated MA...Organo-MMT complex with BMA comonomer: (1) increase of the elastic modulus (from) deleted by more than 16.0 %, i.e., increase of the relaxation temperature from 58.3 up to 67.9°C, (2) increase of the glass transition behavior from 60.1 to

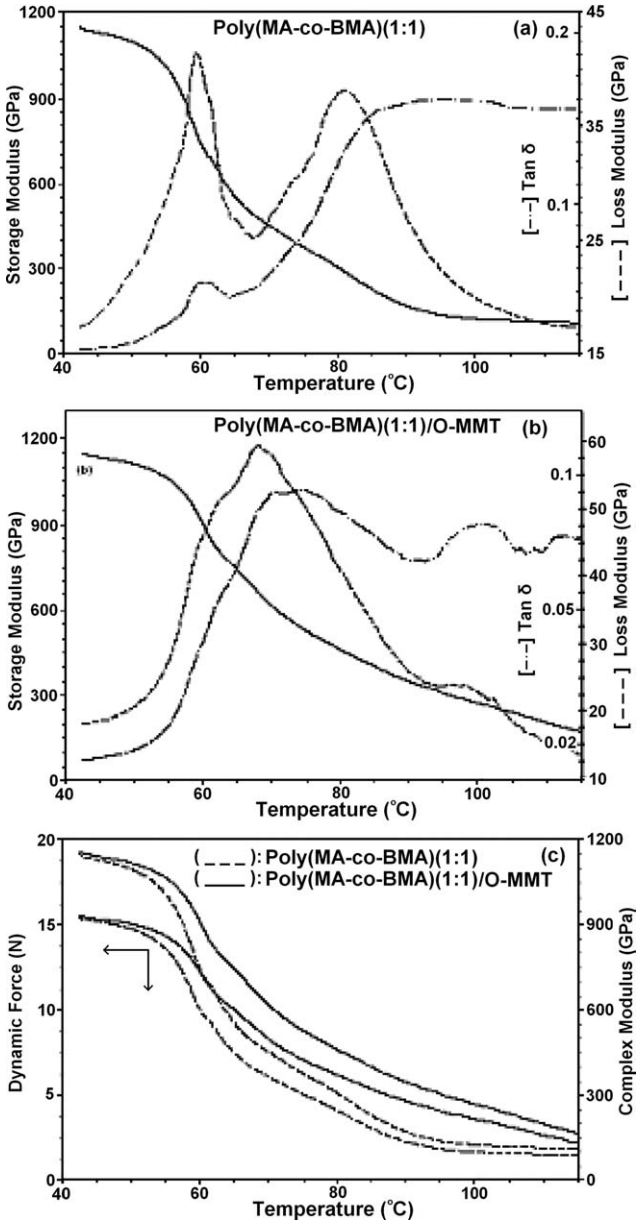

Figure 2 DMA curves of poly(MA-*co*-BMA)-1and its nanocomposite: a plots of (–) SM (G′), (- -) LM (G″), and (- . -) Tan δ G″/G′ vs. temperature for the (a) copolymer and (b) copolymer/O-MMT; (c) plots of CM and DF vs. temperature for the (---) copolymer and (–) copolymer/O-MMT.

74.2°C, (3) unlike pure copolymer, which has two peaks for the flexible BMA segments at 59.3°C and rigid MA units at 80.9°C, respectively, copolymer nanocomposites [Fig. 2(a)] exhibit single broad peak with higher intensity at 67.9°C; the significant increase in intensity of this peak indicates that relaxations of the flexible BMA segments decreased due to the increase of interfacial adhesion strength, i.e., the highest interaction between anhydride units and organo-MMT [Fig. 2(b)]. Dynamic force (DF) and complex modulus (CM) as functions of temperature

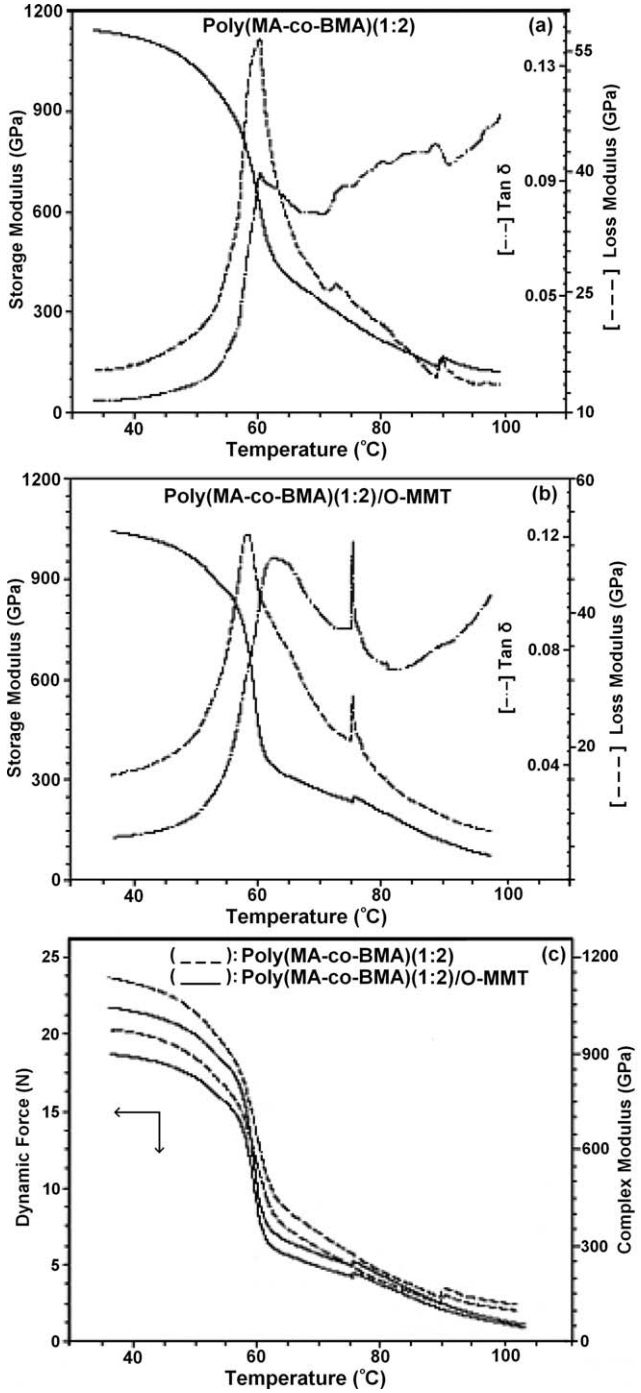

Figure 3 DMA curves of poly(MA-*co*-BMA)-2 and its nanocomposite. Legends as in Figure 2.

and content of flexible BMA unit were illustrated in Figure 2(c). Observed significant difference (Δ) between these parameters [Δ = DF (nanocomposite)–DF(copolymer)] or [Δ = CM(nanocomposite)–CM (copolymer)] above T_g, relating to copolymer and its nanocomposite, can be described (as a function for) due to the formation of nano-structural architecture in poly(MA-*co*-BMA)/organo-MMT system. It can be proposed that Δ value is also characterized by interfacial adhesion strength depending on the flexibility and hydrophobic/hydrophilic balance of the functional polymer chains and their ability to form interfacial complexes. The maximum values of Δ were observed around 85–95°C corresponding to the lower values of DF and CM parameters. It was observed that the character of the

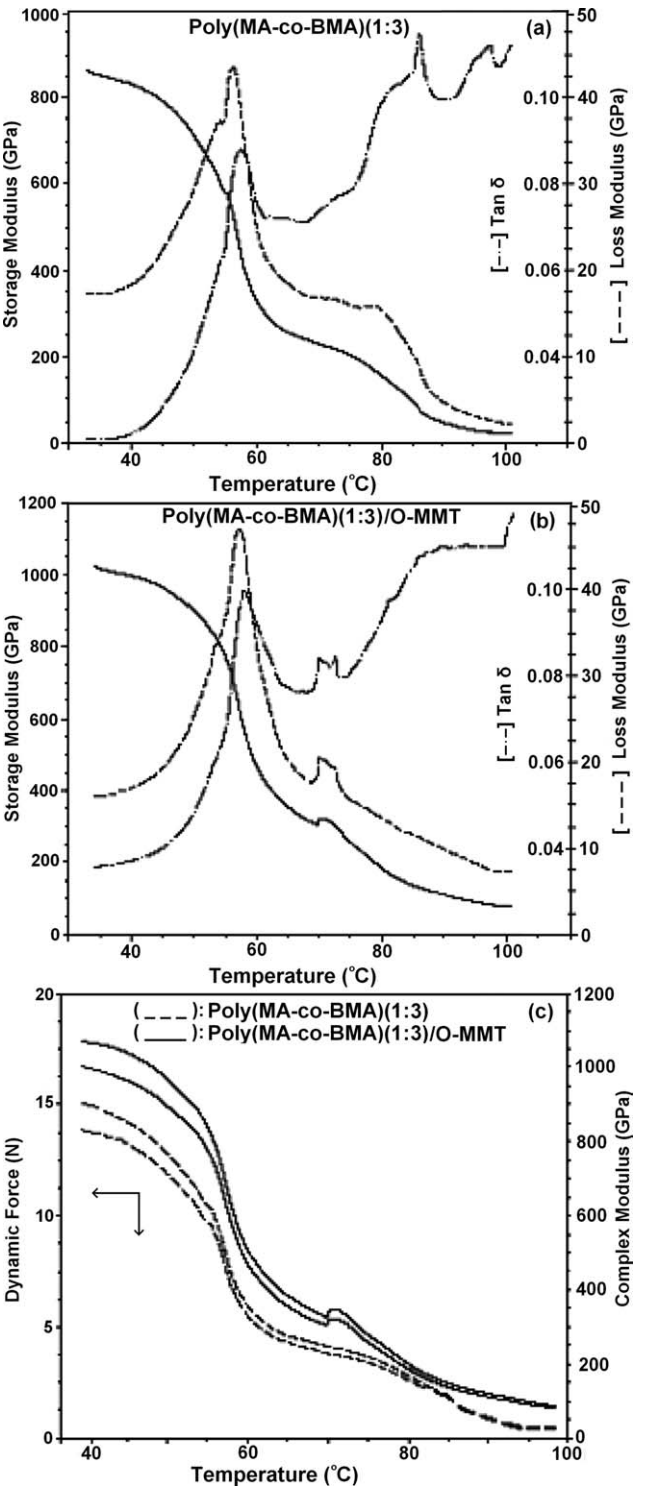

Figure 4 DMA curves of poly(MA-*co*-BMA)-3 and its nanocomposite. Legends as in Figure 2.

TABLE III
DMA Parameters as Functions of BMA Content in Copolymers and Nanocomposites

Copolymers and nanocomposites	BMA (mol %)[a]	DMA parameters[b]: T_α relaxation (°C)					
		T (G' onset)	T (G'' onset)	tan δ (G''/G')	T (DV)	T (FM)	Δ (N) (DF_c–DF_n)
Poly(MA-*co*-BMA)-1	57.2	56.8 80.7	58.3	60.1	59.3	58.3	–
Poly(MA-*co*-BMA)-1/O-MMT	54.4	62.5 98.2	67.9	74.2	67.7	62.8	2.31
Poly(MA-*co*-BMA)-2	85.2	55.3	60.2	60.3	60.2	59.9	–
Poly(MA-*co*-BMA)-2/O-MMT	80.9	57.0 75.2	58.4	62.8	58.6	59.5	1.57
Poly(MA-*co*-BMA)-3	91.8	53.2 79.2	56.4 86.3	57.7 79.2	56.2 87.5	57.2	–
Poly(MA-*co*-BMA)-3/O-MMT	88.2	53.9 70.1	57.3 70.1	58.2 70.2	57.3	57.3	1.83

[a] Copolymer compositions (amount of BMA units) were determined by alkali titration of anhydride units and calculated using eq. (1). Amount of O-MMT is constant (5 wt %).
[b] G', storage modulus; G'', loss modulus; DV is dynamic viscosity; FM is flexural modulus and $\Delta = DF_c - DF_n$ (DF_c and DF_n are dynamic force of copolymer and nanocomposite, respectively).

curves, and therefore, the DMA parameters strongly depend on the amount of flexible *n*-butyl ester linkages in copolymer (Figs. 3 and 4). The obtained DMA parameters were summarized in Table III.

Increase of the BMA unit from 57.2 to 91.6 mol % provides the following changes of DMA curves (Fig. 3): (1) relatively narrow peaks relating to T_g transition (60.2 and 60.3°C for pure copolymer) of the plots of loss modulus (LM) and tan δ vs. temperature transferred to the broad form (T_g = 58.4 and 62.8°C), and intensities of second peaks on the curves at 75.2°C significantly increased, (2) new intensive peak at 86.3°C (is) deleted appeared on the tan δ→temperature curve [Fig. 3(a)], (3) the plots of dynamic force (DF) and complex modulus (CM) vs. temperature [Fig. 3(c)] indicated relatively higher values of Δ before T_g transition, and may be described as degree of exfoliation of copolymer chains. Similar changes are observed in DMA curves for the copolymer containing 91.8 mol % of BMA units (Fig. 4).

However, intensity of the second narrow peaks essentially decreases. These broad peaks also shift to the relatively lower temperature region (70.1°C) [Fig. 4(a)]. These observed unusual changes may be explained by decreasing in force of interfacial interaction due to the reduction of complexed anhydride units in copolymers. Plots of dynamic force (DF) and complex modulus (CM) vs. temperature were illustrated in Figure 4(c). As seen from the character of curves, Δ value significantly increases with increasing content of BMA unit which provides better exfoliation effect in the studied system.

Changes of storage modulus or complex viscosity as a function of flexible BMA unit contents at different temperatures were also investigated. The obtained results are summarized in Table IV. As seen from the DMA analysis data, change in the amount of flexible BMA units in the copolymers and nanocomposites visibly decreased the values of storage modulus and complex viscosity at temperature

TABLE IV
Storage Modulus (SM) and Complex Viscosity (CV) as Functions of Copolymer and Nanocomposite Compositons and Temperature

Copolymers with different contents of flexible BMA units (mol %)[a]	SM (MPa) × 10^5 at (°C)			CV (MPa s) × 10^5 at (°C)		
	45	70	100	45	70	100
Poly(MA-*co*-BMA)-1	11.30	4.51	1.24	0.62	0.25	0.07
Poly(MA-*co*-BMA)-1/O-MMT	11.42	6.13	2.69	0.63	0.34	0.15
Poly(MA-*co*-BMA)-2	10.90	3.39	0.14	0.60	0.19	0.07
Poly(MA-*co*-BMA)-2/O-MMT	10.07	2.70	0.63	0.56	0.15	0.04
Poly(MA-*co*-BMA)-3	7.92	2.28	0.21	0.44	0.13	0.01
Poly(MA-*co*-BMA)-3/O-MMT	9.65	3.17	0.79	0.53	0.17	0.04

[a] Content of BMA units as in Table III.

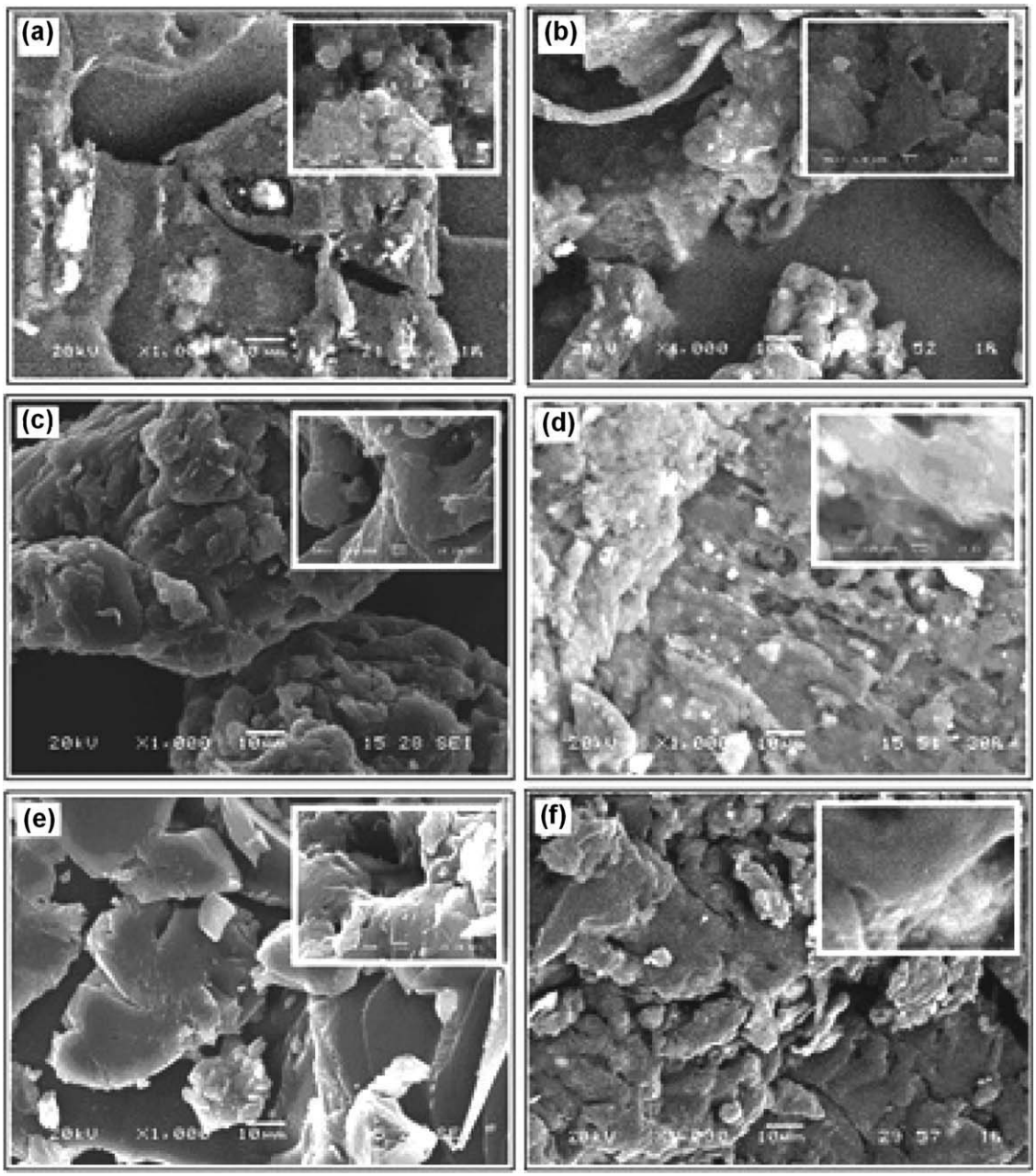

Figure 5 SEM patterns (scale: 1 and 10 μm, x1000 magnification): (a) poly(MA-*co*-BMA)-1, (b) poly(MA-*co*-BMA)-1/O-MMT, (c) poly(MA-*co*-BMA)-2, (d) poly(MA-*co*-BMA)-2/O-MMT, (e) poly(MA-*co*-BMA)-3, and (f) poly(MA-*co*-BMA)-3/DMDA-MMT.

interval changing from 45 to 100°C. These observed changes were exhibited at relatively higher values of storage modulus for the nanocomposites due to their rigid structures when compared with virgin copolymers. Similar effect of BMA content and temperature was observed for the other DMA parameters of the copolymers and copolymers/O-MMT nanocomposites (Figs. 2–4). These observations indicate that a degree of physical structural change depends on the content of flexible *n*-butyl ester linkages and temperature. An increase in the number of BMA units in the preintercalated MA...O-MMT complex monomer/comonomer feed, which leads to the internal plasticization effect in copolymer/O-MMT nanocomposites, essentially facilitates the exfoliation process of the copolymer chains forming through interlamellar copolymerization. On the other hand, the better compatibility of the preintercalated complex with BMA monomer and O-MMT clay tends to favor the disentanglement of bundles and provides the relatively fine dispersion of copolymer/O-MMT hybrid system.

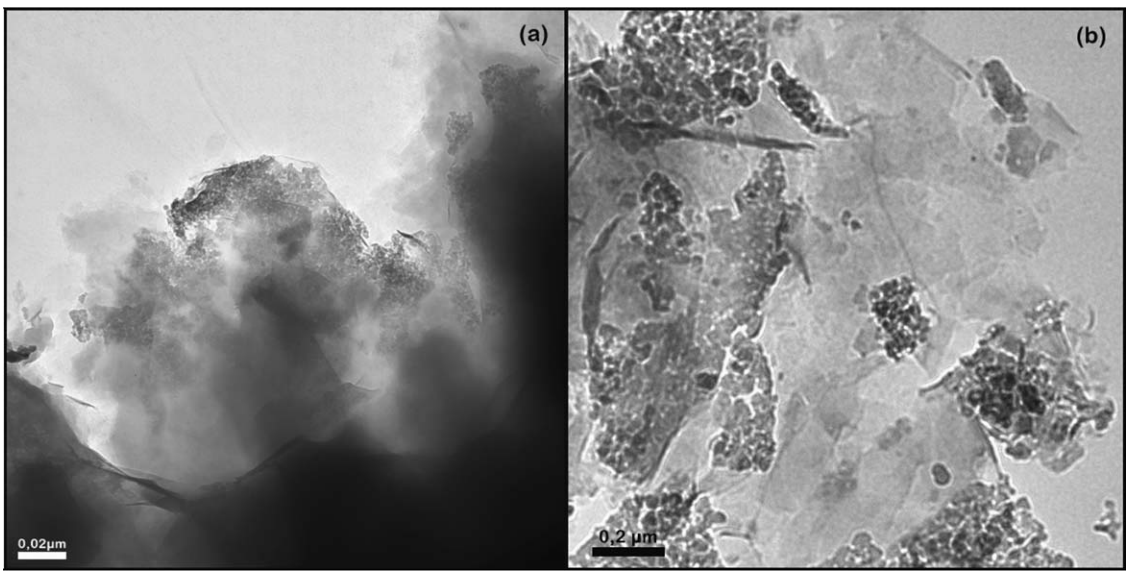

Figure 6 TEM micrographs of poly(MA-*co*-BMA)/O-MMT-2: scale (a) 0.02 μm, × 40.000 and (b) 0.2 μm, × 20.000 magnification.

Morphology of nanocomposites

Figure 5 shows the SEM image of the poly(MA-*co*-BMA)s containing different amounts of BMA units and their nanocomposites prepared by interlamellar copolymerization. SEM images of these hybrid composites inferred that the size of the particles significantly depends on the content of flexible BMA linkages and *in situ* complex formation. An increase of BMA content in copolymers provides the facile exfoliation of polymer chains into DMDA-MMT galleries and formation of relatively high dispersed particles. In the case of copolymer nanocomposite [Fig. 5(e)], containing at most BMA segments and therefore, least amount of preintercalated MA...O-MMT complexes, the formation of well dispersed particles was observed due to the easily exfoliated BMA chain blocks between silicate galleries.

We have observed that the compatibility of the chosen BMA monomer and a long alkyl group of intercalated DMDA-clay, the MA monomer, and an alkyl ammonium cation (through complex formation) plays an important role *in situ* intercalation/exfoliation of copolymer chains between silicate layers. The observed reduction of T_g value as a function of the BMA linkage content can be explained by the internal plasticizing effect of flexible butyl ester branches. Similar effect was observed by Qi et al.[36] in the free-radical *in situ* intercalative bulk polymerization of styrene in the presence of organophilic (benzyldimethyloctadecylammonium cation) MMT. They demonstrated that the structural affinity between the styrene monomer and the benzyl group of intercalated surfactant-MMT is an important factor for the preparation of polystyrene/clay nanocomposites with higher molecular weights and a higher thermal stability. According to the authors, the TEM analysis of nanocomposites morphology indicated the formation of the mixture exfoliated (predominantly) and partially intercalated structure. It can be proposed that this is an important factor to explain the observed higher thermal stability of the PS-clay nanocomposites. The results obtained by several researchers from the comparative TEM and thermal analysis of polymer/clay hybrids, such as polypropylene/polystyrene,[37] poly(styrene-*co*-acrylonitrile),[38] and poly(etherimide)[39] silicate layered nanocomposites, indicated that the completely exfoliated structure exhibits relatively lower thermal stability than nanosystem with a mixture intercalated/exfoliated structure.

To further confirm the dispersion of organoclay in the matrix copolymer, TEM investigation is also required. According to Monticelli et al.,[40] TEM analysis method turns out to be less challenging when exfoliated nanocomposites are studied with respect to the characterization of intercalated nanostructure systems, where clay structure undergoes a modification and decomposition under electron beams, which is evidenced by the disappearance of some layers and the toning down of others. Thus, for preparing TEM specimens of the copolymer/organoclay nanocomposite, the focused ion beam technique was used with a shorter time exposition around 10–20s. TEM micrographs of the poly(MA-*co*-BMA)/organoclay nanocomposites were illustrated in Figure 6. It can be seen from the TEM images that the separation of clay layers seemed to be highly efficient in nanocomposites system. Some aggregation of the clay layers in the nanosystem were observed to exhibit better intercalation/exfoliation copolymer chains between silicate galleries. The presence of

single clay layers homogenously dispersed in copolymer matrix indicates the formation of individual dispersion of delaminated clay platelets, and therefore a completely exfoliated nanostructure in poly(MA-*co*-BMA)/organoclay nanocomposites due to interfacial interaction via strong complex formation. Relatively homogenous phase distribution observed for this nanocomposite is reasonably in agreement with XRD and SEM analysis results.

CONCLUSIONS

This work presents a new approach to synthesize functional copolymer/organoclay nanocomposites by complex-radical interlamellar copolymerization of preintercalated MA…O-MMT complex as a 'nano-reactor' with BMA comonomer as internal plasticizing agent. The results of the comparative XRD and DMA analyzes of copolymers and their nanocomposites indicate that the observed effects of interlayer complex formation and internal plasticization of the flexible *n*-butyl ester linkages play an important role in interlamellar copolymerization and intercalation/exfoliation *in situ* processes, in the local chain folding, and in crystallization process. In general, an increase in the amount of flexible *n*-butyl ester linkages leads to significantly lower T_g values, and therefore, to an easier exfoliation process of copolymer chains into organoclay galleries due to the internal plasticization effect of BMA units. On the other hand, complex formation between MA units and ammonium cations of organoclay layered surface increases the force of interfacial interaction between organic (copolymer chains) and inorganic phases. This preintercalated complex also plays an important role as a reactive compatibilizer in the formation of nano-structural architectures with given thermal and dynamic mechanical properties. Synthesized hybrids may be utilized as nano-films and nano-coatings in the in-line coating processing for surface modification of various thermoplastic films, as reactive compatibilizer-nanofillers for the reactive thermoplastic polymer blends, especially for the acrylic polymer based systems, and also as components of the various nanomaterials prepared in melt by reactive extrusion *in situ* processing.

The authors thank the Turkish Scientific and Technical Research Council (TÜBİTAK) and Science and Research Unit (BAB) of Hacettepe University for the financial supports of this work through Projects TBAG-HD/249 and BAB(DPT)-K120930, respectively.

References

1. Söylemez, E.; Çaylak, N.; Rzayev, Z. M. O. eXPRESS Polym Lett 2008, 2, 639.
2. Rzayev, Z. M. O.; Yilmazbayhan, A.; Alper, E. Adv Polym Technol 2007, 26, 41.
3. Rzayev, Z. M. O. Nanotechnology methods in polymer engineering, In Proceedings of 4th Nanoscience & Nanotechnology Conference; Bilkent, Ankara-Turkey, **June** 11–14, 2007; p 154.
4. Rzayev, Z. M. O.; Can, H. K.; Güner, A. J Appl Polym Sci 2003, 90, 4009.
5. Rzayev, Z. M. O.; Güner, A.; Can, H. K.; Aşici, A. Polymer 2001, 42, 5599.
6. Zeng, Q. H.; Wang, D. Z.; Lu, G. Q. Nanotechnology 2002, 13, 549.
7. Uthirakumar, P.; Nahm, K. S.; Hahn, Y. B.; Lee, Y. S. Eur Polym J 2004, 40, 2437.
8. Liu, G. D.; Zhang, L. C.; Zhao, D. G.; Qu, X. G. J Appl Polym Sci 2005, 96, 1146.
9. Biswas, M.; Ray, S. S. Polymer 1998, 39, 6423.
10. Friedlander, H. Z. ACS Polym Prepr 1963, 4, 300.
11. Solomon, D. H.; Loft, B. C. J Appl Polym Sci 1968, 12, 1253.
12. Nese, A.; Sen, S.; Tasdelen, M. A.; Nugay, N.; Yagci, Y. Macromol Chem Phys 2006, 207, 820.
13. Lee, D. C.; Jang, L. W. J Appl Polym Sci 2005, 96, 1117.
14. Liu, G. D.; Zhang, L. C.; Qu, X. W.; Wang, B. T.; Zhang, Y. J Appl Polym Sci 2003, 90, 3690.
15. Stadtmueller, L. M.; Ratinac, K. R.; Ringer, S. P. Polymer 2005, 46, 9574.
16. Sugahara, Y.; Satokawa, S.; Kuroda, K.; Kato, C. Clays Clay Miner 1988, 36, 343.
17. Li, H. M.; Chen, H. B. Mater Lett 2003, 57, 3000.
18. Vaysse, C.; Guerlou-Demourgues, L.; Delmas, C.; Duguest, E. Macromolecules 2004, 37, 45.
19. Vaysse, C.; Guerlou-Demourgues, L.; Duguet, E.; Delmas, C. Inorg Chem 2003, 42, 4559.
20. Vieille, L.; Taviot-Gueho, C.; Besse, J. P.; Leroux, F. Chem Mater 2003, 15, 4369.
21. Vieille, L.; Moujahid, E. M.; Taviot-Gueho, C.; Cellier, J.; Besse, J. P.; Leroux, F. J Phys Chem Solids 2004, 65, 385.
22. Yu, F.; Yao, K.; Shi, L.; Wan, W.; Zhong, Q.; Fu, Y.; You, X. Chem Mater 2007, 19, 3412.
23. Moujahid, E. M.; Dubois, M.; Besse, J. P.; Leroux, F. Chem Mater 2002, 14, 3799.
24. Al-Esaimi, M. M. J Appl Polym Sci 1997, 64, 367.
25. Liu, G. D.; Zhang, L. C.; Gao, C. H.; Qu, X. G. J Appl Polym Sci 2005, 98, 1932.
26. Liu, G. D.; Zhang, L. C.; Qu, X. G.; Liu, P.; Yang, L.; Gao, C. H. J Appl Polym Sci 2002, 83, 417.
27. Wang, D.; Zhu, J.; Yao, Q.; Wilkie, C. A. Chem Mater 2002, 14, 3837.
28. Wang, D.; Zhu, J.; Wilkie, C. A. Polym Degrad Stab 2003, 80, 171.
29. Tjong, S. C. Mater Sci Eng 2006, 53, 73.
30. Nguyen, Q. T.; Baird, D. G. Adv Polym Technol 2006, 25, 270.
31. Heinz, H.; Vaia, R. A.; Krishnamoorti, R.; Farmer, B. L. Chem Mater 2007, 19, 59.
32. Gong, X.; Liu, J.; Baskaran, S.; Voise, R. D.; Young, J. S. Chem Mater 2000, 12, 1049.
33. Roe, R. J. In Encyclopedia of Polymer Science and Engineering, 2nd ed.; Mark, H. F., Bikales, N. M., Overberger, C. C., Menges, G., Eds. ; John Wiley & Sons: New York, 1987; p 542.
34. Sperling, L. H. Introduction to Physical Polymer Science; 2nd ed.; John Wiley & Sons: New York, 1992; p 370.
35. Masenelli-Varlot, K.; Vigier, G.; Vermogen, A. J Polym Sci Part B: Polym Phys 2007, 45, 1244.
36. Qi, R.; Jin, X.; Nie, J.; Yu, W.; Zhou, C. J Appl Polym Sci 2005, 97, 201.
37. Gilman, W.; Jakson, C. L.; Morgan, A. B.; Harris, R. H.; Manias, E.; Giannelis, E. P.; Wuthenow, M.; Hilton, D.; Philip, S. H. J Chem Mater 2000, 12, 1866.
38. Cai, Y.; Hu, Y.; Xiao, J.; Song, L.; Fan, W. Polym Plast Technol Eng 2007, 46, 541.
39. Lee, L.; Takekoshi, T.; Giannelis, E. P. Mater Res Soc Symp Proc 1997, 457, 513.
40. Monticelli, O.; Musina, Z.; Russo, S.; Bals, S. Mater Lett 2007, 61, 3446.